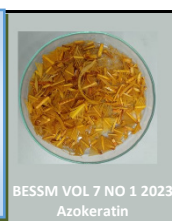


BULLETIN OF ENVIRONMENTAL SCIENCE & SUSTAINABLE MANAGEMENT

Website: <http://journal.hibiscuspublisher.com/index.php/BESSM/index>



Exploring the Influence of Azo Dye Congo Red on *Acinetobacter baumannii* YNWH 226 Growth: A Secondary Modeling Study

Ibrahim Alhaji Sabo¹, Salihu Yahuza², Bilal Ibrahim Dan-Iya³, Abdussamad Abubakar⁴, Tasiu Mahmud⁵, Dauda Danlami⁶ and Mohd Ezuan Khayat^{7*}

¹Department of Microbiology, Faculty of Pure and Applied Sciences, Federal University Wukari, P.M.B. 1020 Wukari, Taraba State, Nigeria.

²Department of Microbiology and Biotechnology, Faculty of Science, Federal University Dutse, P.M.B., 7156, Dutse, Jigawa State, Nigeria.

³Department of Pharmacy Technician, College of Health Sciences, Kano, and Technology, Kano, Nigeria

⁴National Environmental Standards and Regulations Enforcement Agency, P.M.B. 641, Wuse Zone 7, NESREA, Abuja, FCT, Nigeria.

⁵Department of Microbiology, Faculty of Sciences, Kano University of Science and Technology, Wudil. P.M.B. 3244, Kano State, Nigeria

⁶Department of Biotechnology, Faculty of Science, Federal University Lokoja, P.M.B. 1154, Lokoja, Kogi State, Nigeria.

⁷Department of Biochemistry, Faculty of Biotechnology and Biomolecular Sciences, Universiti Putra Malaysia, 43400 UPM Serdang, Selangor, Malaysia.

*Corresponding author:

Mohd Ezuan Khayat,

Department of Biochemistry,

Faculty of Biotechnology and Biomolecular Sciences,

Universiti Putra Malaysia, 43400 UPM Serdang,

Selangor,

Malaysia.

Email: m_ezuan@upm.edu.my

HISTORY

Received: 4th April 2023
Received in revised form: 12th July 2023
Accepted: 30th July 2023

KEYWORDS

Biodegradation
Congo red
Inhibition kinetics
Azo dye
Acinetobacter baumannii

ABSTRACT

One of the challenges that face the textile industry is the release of effluents that are not wanted, most notably colors that do not degrade. This is one of the issues that plagues the industry. This is a concern since it affects the environment. Bioremediation using dye-degrading bacterium is appealing as bacterial metabolism converts hazardous dye to harmless carbon dioxide and water as byproducts. In this study, various secondary growth models such as Luong, Yano, Teissier-Edward, Aiba, Haldane, Monod, Han, and Levenspiel were employed. Following thorough statistical analyses such as root-mean-square error (RMSE), adjusted coefficient of determination ($\text{adj}R^2$), bias factor (BF), and accuracy factor (AF), the Luong model emerged as the most optimal choice. The half-saturation constant for maximal growth, maximal growth rate and maximal concentration of substrate tolerated and curve parameter that defines the steepness of the growth rate decline from the maximum rate symbolized by K_s , μ_{max} and S_m , and n were 8.023 mg/L (95% C.I., -153.852 to 169.898), 0.437 per d (95% C.I., -0.121 to 0.995), 551.629 mg/L (95% C.I., 378.823 to 724.435) and 3.907 (95% C.I., -8.808 to 16.621), respectively. These novel constants discovered during the modeling process could serve as valuable inputs for subsequent modeling pursuits.

INTRODUCTION

The textile sector contributes positively to global economic development. China leads as the primary exporter of various textile goods, with the European Union, India, and the USA following in that order. However, an issue that plagues textile factories is the release of undesirable effluents, particularly non-degradable dyes, posing a difficult problem [1]. Dye pollutants consist of a range of toxic and non-degradable components that have the potential to disturb the delicate balance of aquatic ecosystems. Such disruption can harm aquatic organisms, interfere with the intricate web of food chains, and ultimately result in a decline in biodiversity [2,3]. Human health can be adversely affected by dye pollutants, which may contain

carcinogenic and mutagenic compounds. Contact with contaminated water may result in health issues, such as skin irritation and respiratory problems [4]. A key challenge to the current conventional water treatment systems is the rapidly increasing amount of hazardous dye wastewater generated by various sectors. This is a critical public health concern as well as an environmental one. Consequently, a range of physico-chemical and biological treatment techniques have been studied, with different removal capacities contingent upon the limitations of the experiments. [3].

Biological treatment techniques for removing toxic dyes are both affordable and environmentally friendly, generating minimal sludge. Microbial technology is increasingly being

recognized as an effective alternative for addressing this issue [3,5]. Various types of bacteria, with their ease of cultivation and quick growth, are well-suited for efficiently breaking down dyes. Research on the degradation of dyes by bacteria dates back to the 1970s, with initial strains like *Bacillus subtilis*, *Aeromonas hydrophila*, and *B. cereus* found to have the capability to decolorize azo dyes [5]. Congo red, an azo dye, is frequently found as a co-pollutant. Approximately one million tons of basic and diazo direct dyes are manufactured each year. According to the Ecological and Toxicological Association of the Dyestuff Manufacturing Industry (ETAD), it is identified as having the most elevated toxicity levels [6].

The azo dye contains a chromophoric azo group (N=N), which imparts color to the materials. Depending on the quantity of azo groups they contain, azo dyes can be categorized as monoazo, diazo, or polyazo dyes. It can also be classified into various categories, including direct, reactive, dispersion, metalized, cationic, and anionic azo dyes, based on their specific applications [7]. *Acinetobacter baumannii* has displayed its ability to break down a variety of synthetic dyes and organic pollutants in both wastewater and natural environments. Its capacity to adapt to diverse environmental conditions and its enzymatic machinery for processing complex compounds position it as a promising contender for bioremediation procedures.

The involvement of this bacterium in dye degradation can contribute significantly to reducing water pollution and remediating contaminated areas [8,9]. Mathematical modeling techniques were utilized, incorporating data from Fig. 2 of Xun-an Ning, et. al [10]. Numerous research studies have introduced various substrate inhibition kinetics models for the degradation of pollutants such as Haldane, Monod, Yano and Koga, Aiba, Teissier, Luong and Han, and Levenspiel [11–20].

MATERIALS AND METHODS

Data acquisition

The graphical data extracted from Figure 1a in the research conducted by Xun-an Ning et al. [10] on Decolorization and Biodegradation of the Azo Dye Congo Red by an Isolated *Acinetobacter baumannii* YNWH 226, was analyzed using the software tool Webplot digitizer. This software is widely acknowledged and embraced within the scientific community [21], for its capacity to convert scanned figures into digital data. Its precision and reliability have been consistently recognized by numerous researchers [22,23].

The data was further analyzed and modeled using Curve Expert Professional software (Version 2.6.5) to elucidate the scientific insights and trends within the dataset, contributing to the robustness of the study's findings. This combination of data digitization and advanced software analysis is a common and essential practice in modern scientific research, ensuring the accuracy and validity of results.

Fitting of the data

The Marquardt algorithm was employed for nonlinear regression to fit various bacterial growth models (Table 1) and this analysis was conducted using Curve Expert Professional software (Version 2.6.5). The algorithm aims to find the most optimal method for minimizing the sum of squares between predicted and observed values. In this process, the software can be configured manually or automatically to determine the initial parameter

values, and the steepest gradient search between the four data points was utilized to estimate the maximum growth rate (μ_{max}).

Statistical analysis

The statistically significant difference between the models was evaluated using various metrics. The following statistical functions were utilized to determine the best models;

The RMSE allows number of parameters' penalty and was calculated using Equation 1, where n illustrates the number of experimental data, where else p is the number of parameters calculated by the model and experimental data and values predicted by the model are Ob_i and Pd_i , respectively [24]. With the regression line approaching the data points, the root mean square error (RMSE) reduces due to the reduced error in the model. More accurate predictions are generated by a model that has a lower error rate. Comparable in magnitude to the dependent (outcome) variable, the RMSE values span an infinite number of positive infinities. The root mean square error (RMSE) can be employed to assess the extent of imprecision in a statistical model, including regression models. If a value is zero, it signifies that the predicted and actual values are an exact match. The model exhibits superior data fit and generates more precise predictions, as indicated by low RMSE values. In contrast, increased levels indicate a greater magnitude of errors and a reduced number of precise predictions.

$$RMSE = \sqrt{\frac{\sum_{i=1}^n (Pd_i - Ob_i)^2}{n-p}} \quad (\text{Eqn. 1})$$

The R^2 value, also known as the coefficient of determination, was used in linear regression to select the model that provided the best fit. On the other hand, in the case of nonlinear regression, the R^2 does not provide a comparative analysis in situations in which the number of parameters in the various models varies. In order to get around this obstacle, the quality of the nonlinear models was determined by adjusting the R^2 value. S_y^2 is the total variance of the y-variable, while RMS stands for residual mean square. These two terms are used in the adjusted R^2 formula (Equations 2 and 3).

$$\text{Adjusted } (R^2) = 1 - \frac{RMS}{S_y^2} \quad (\text{Eqn. 2})$$

$$\text{Adjusted } (R^2) = 1 - \frac{(1-R^2)(n-1)}{(n-p-1)} \quad (\text{Eqn. 3})$$

One can measure the relative quality of various statistical models for a given set of experimental data by using the Akaike Information Criterion (AIC). This criterion was developed by Akaike. Instead, data sets that have a large number of parameters or few values should utilize the AIC that has been corrected, which is denoted by the letter AICc [25]. The AICc was determined using the equation that is presented below (Equation 4).

$$AICc = 2p + n1n \left(\frac{RSS}{n} \right) + 2(p+1) + \frac{2(p+1)(p+2)}{n-p-2} \quad (\text{Eqn. 4})$$

Another statistical measure that is founded on information theory is known as the Bayesian Information Criterion (BIC) (Equation 5), which can be compared to the AICc. Models with the lowest Bayesian information criterion (BIC) are typically preferred over those with higher BICs when choosing from a finite number of models. It has close ties to the Akaike information criteria and is partially based on the likelihood function (AIC). This error function imposes a harsher penalty on the number of parameters than the AIC does [26].

$$BIC = n \cdot \ln \frac{RSS}{n} + p \cdot \ln(n) \quad (\text{Eqn. 5})$$

The Hannan–Quinn information criterion, often known as the HQC, is an additional error function approach that is based on the information theory (Equation 7). To evaluate how well a statistical model fits data, experts use the Hannan–Quinn information criterion (HQC). It is a common metric to employ when choosing one model over another. In contrast to the LLF, it is connected to Akaike's information criterion. The HQC, like the AIC, includes a penalty function for the total number of model parameters, however it is significantly bigger than the value assigned by the AIC because the equation contains the $\ln \ln n$ term [27];

$$HQC = n \times \ln \frac{RSS}{n} + 2 \times p \times \ln(\ln n) \quad (\text{Eqn. 7})$$

Both BF and AF were utilized in an effort to evaluate the appropriateness of the models. In order to get a correlation of 1 between the anticipated value and the observed value, the Bias Factor needs to be equal to 1.

The Bias Factor and Accuracy Factor originates from predictive microbiology under the food microbiology field and have found applications in modelling microbial growth that leads to food spoilage [28–35]. A fail-safe model is indicated when the value of the Bias Factor (Equation 8) is greater than 1, and a fail-negative model is indicated when the value of the Bias Factor is less than 1. When compared to 1, a value of Accuracy that is less than 1 indicates a less accurate prediction (Equation 9).

$$\text{Bias factor} = 10 \left(\sum_{i=1}^n \log \frac{(Pd_i/Ob_i)}{n} \right) \quad (\text{Eqn. 8})$$

$$\text{Accuracy factor} = 10 \left(\sum_{i=1}^n \log \frac{|(Pd_i/Ob_i)|}{n} \right) \quad (\text{Eqn. 9})$$

Another parameter-penalized model is MPSD. The Marquardt's percent standard deviation (MPSD). This error function distribution follows the geometric mean error which allows for the penalty to the number of parameters of a model (Equation 10).

$$MPSD = 100 \sqrt{\frac{1}{n-p} \sum_{i=1}^n \left(\frac{Ob_i - Pd_i}{Ob_i} \right)^2} \quad (\text{Eqn. 10})$$

where p is the number of parameters, n is the number of experimental data, Ob_i is the experimental data, and Pd_i is the value predicted by the model.

RESULTS AND DISCUSSION

The strategies for diminishing dye pollution involve the innovation of sustainable dyes, the advancement of wastewater treatment methods, and the dissemination of knowledge about the ecological implications of the textile and dye sectors. According to the analysis of the bacterial growth model, as depicted in **Figs. 1 to 7**.

All of the studied models showed good fittings except Moser, Monod which has the poorest curve fitting. The Han-Levenspiel model failed to converge and was omitted from the data analysis. The Luong model emerged as the most suitable model, as indicated by its remarkably low values for RMSE, AICc, and modified $\text{adj}R^2$. Furthermore, the model's AF and BF values were particularly outstanding (**Table 2**).

The half-saturation constant for maximal growth, maximal growth rate and maximal concentration of substrate tolerated and curve parameter that defines the steepness of the growth rate decline from the maximum rate symbolized by K_s , μ_{max} and S_m , and n were 8.023 mg/L (95% C.I., -153.852 to 169.898), 0.437 per d (95% C.I., -0.121 to 0.995), 551.629 mg/L (95% C.I., 378.823 to 724.435) and 3.907 (95% C.I., -8.808 to 16.621), respectively. The large range for the confidence interval indicates more data points are needed and the fitting was not adequate. The luong model has an advantage compared to the simple Monod or Haldane model in the fact that it could predict substrate concentration that can completely inhibited growth rate.

These parameters are a valuable resource for researchers and practitioners seeking to apply the simple Monod model. While the Monod model offers benefits, it is crucial to note that its relevance might be constrained in certain situations. For instance, it assumes a consistent specific growth rate, which may not hold in dynamic environments. In such cases, more intricate models that address factors like substrate inhibition or the presence of multiple limiting nutrients could be more fitting. The choice of the optimal model depends on the unique characteristics of the microbiological system being studied and the data at hand.

Table 1. Various mathematical models developed for degradation kinetics involving substrate inhibition.

Author	Degradation Rate	Author
Monod	$\frac{\mu_{max} S}{S + K_s}$	[36]
Haldane	$\frac{\mu_{max} S}{S + K_s + \left(\frac{S^2}{K_i}\right)}$	[37]
Teissier	$\mu_{max} \left(1 - \exp\left(-\frac{S}{K_i}\right) - \exp\left(\frac{S}{K_s}\right) \right)$	[38]
Aiba	$\mu_{max} \frac{S}{K_s + S} \exp\left(-\frac{S}{K_i}\right)$	[39]
Yano and Koga	$\frac{\mu_{max} S}{S + K_s + \left(\frac{S^2}{K_i}\right) \left(1 + \frac{S}{K}\right)}$	[40]
Han and Levenspiel	$\mu_{max} \left(1 - \left(\frac{S}{S_m}\right) \right)^n \left(\frac{S}{S + K_s \left(1 - \left(\frac{S}{S_m}\right) \right)^m} \right)$	[41]
	$\mu_{max} \frac{S}{S + K_s} \left(1 - \left(\frac{S}{S_m}\right) \right)^n$	[42]
Luong	$\frac{\mu_{max} S^n}{K_s + S^n}$	[43]
Moser	$\frac{\mu_{max} S \left(1 + \frac{S}{K} \right)}{S + K_s + \frac{S^2}{K_i}}$	[44]
Webb	$\frac{\mu_{max} S}{S + K_s + \frac{S^2}{K_i}}$	
Hinshelwood	$\mu_{max} \frac{S}{K_s + S} (1 - K_p P)$	[45]

Note:
 μ_{max} maximal specific growth rate
 K_s half saturation constant
 K_i inhibition constant
 S_m maximal concentration of substrate tolerated
 K_p product inhibition constant
 m, n, K curve parameters
 S substrate concentration
 P product concentration

Table 2. Statistical analysis of the various models used in this study.

Model	<i>p</i>	RMSE	adR ²	MPSD	AICc	BIC	HQC	BF	AF
Luong	4	0.04	0.88	158.11	n.a.	-37.39	-39.89	1.004	1.056
Yano	4	0.07	0.67	29.61	n.a.	-31.85	-34.35	1.029	1.122
Tessier-Edward	3	0.05	0.87	21.62	13.69	-34.93	-36.81	1.029	1.108
Aiba	3	0.05	0.87	21.61	13.69	-34.93	-36.81	1.029	1.108
Haldane	3	0.07	0.71	27.58	17.53	-31.09	-32.97	1.055	1.154
Monod	2	0.13	-0.61	45.68	-4.53	-22.95	-24.20	0.977	1.361
Han and Levenspiel	5	n.a.	n.a.	n.a.	n.a.	n.a.	n.a.	n.a.	n.a.
Moser	3	0.16	-1.41	52.75	27.47	-21.15	-23.03	0.977	1.361
Hinshlewood	4	0.14	-0.99	47.25	n.a.	-22.73	-25.23	1.059	1.257
Webb	4	0.08	0.43	33.78	n.a.	-29.30	-31.80	1.055	1.154

Note: *p*: number of parameters

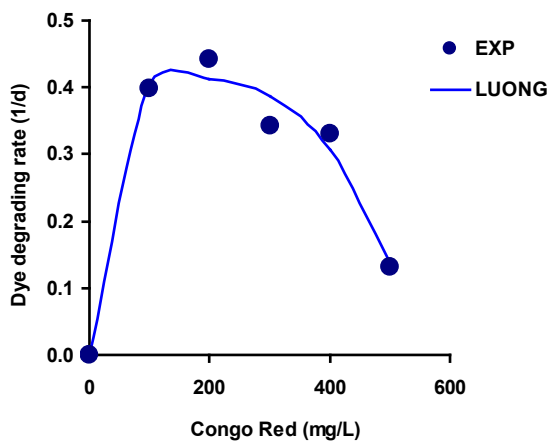


Fig. 1. Growth of *Acinetobacter baumannii* YNWH 226 modeled using Luong.

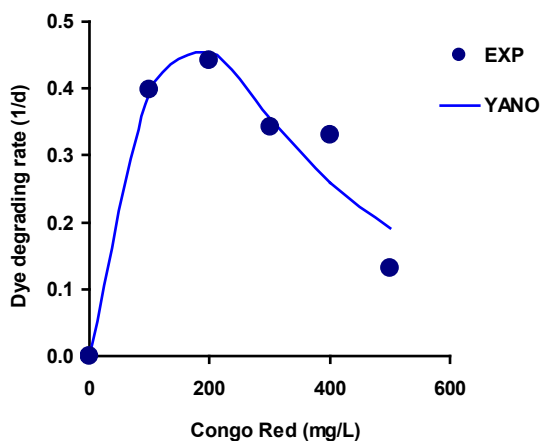


Fig. 2. Growth of *Acinetobacter baumannii* YNWH 226 modeled using Yano.

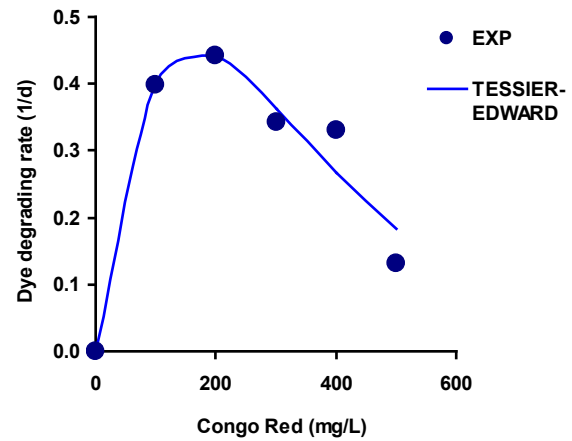


Fig. 3. Growth of *Acinetobacter baumannii* YNWH 226 modeled using Tessier- Edward.

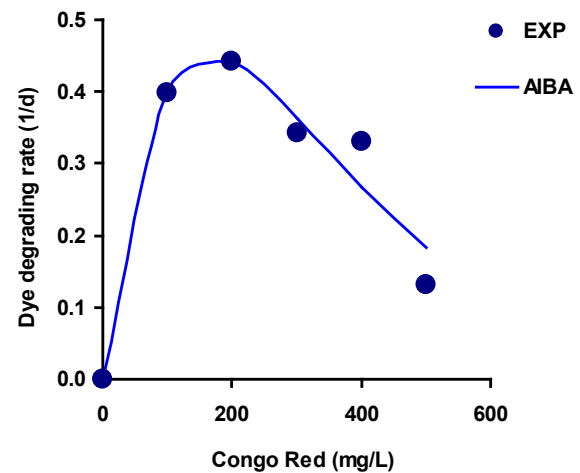


Fig. 4. Growth of *Acinetobacter baumannii* YNWH 226 modeled using Aiba.

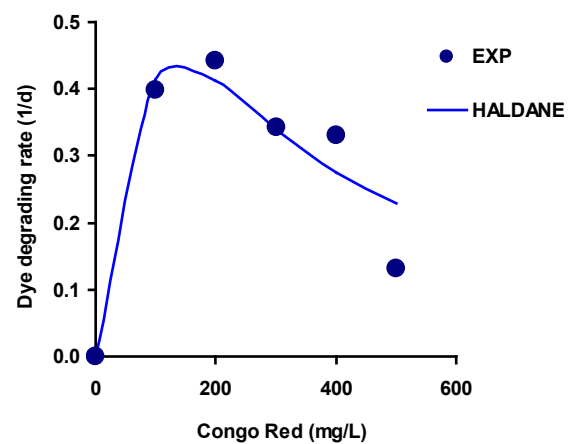


Fig. 5. Growth of *Acinetobacter baumannii* YNWH 226 modeled using Haldane.

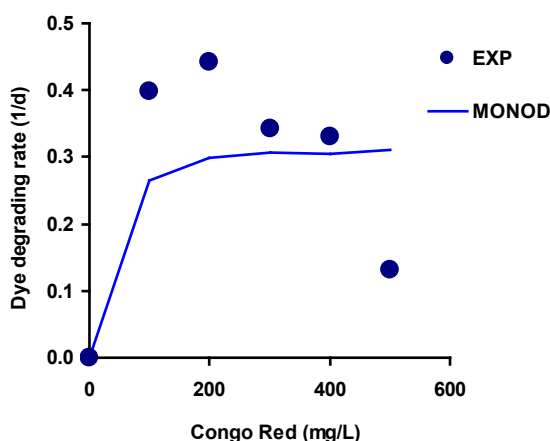


Fig. 6. Growth of *Acinetobacter baumannii* YNWH 226 modeled using Monod.

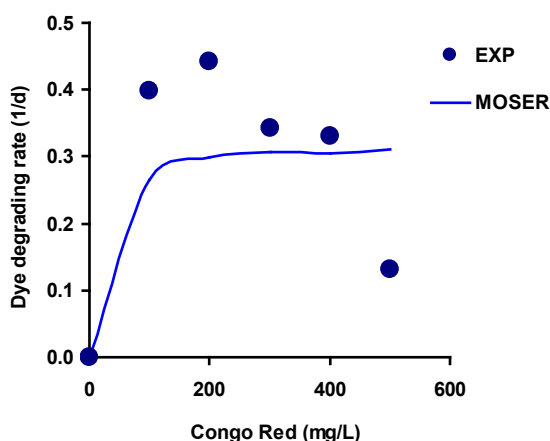


Fig. 7. Growth of *Acinetobacter baumannii* YNWH 226 modeled using Han-Levenspiel.

In practical terms, these biologically meaningful coefficients obtained from the analysis will be highly valuable for guiding and enhancing batch and field experiments. They will allow researchers and environmental scientists to make accurate predictions regarding the growth conditions and needs of *Acinetobacter baumannii* YNWH 226 when employed for the remediation of Azo dye Congo red in polluted environments. The use of substrate inhibition kinetics model in assessing the toxicity of dyes to the growth or degradation rate of microorganisms is beginning to be recognized as an important exercise. For instance, *Anoxybacillus* sp. PDR2 was able to decolorize different azo dyes in the descending order of Congo red > Direct Black 38 > Amaranth > DBG > Methyl Orange with Haldane modelling yielding yielded a maximum degradation rate or q_{max} from 3.331 to 13.592 h^{-1} at dyes concentrations from 149.014 to 340.642 mg/L, respectively [46].

Sonolysis was used as pretreatment for another investigation on Congo Red biodegradation, and then a biological treatment employing an isolated and acclimatized strain of *Bacillus* sp. acquired from tannery industry effluent was used. Using the Haldane model, a q_{max} , K_s and K_i values of 0.4237 h^{-1} , 177 mg/L and 557 mg/L, were obtained [47]. In another study, soil samples taken near a textile plant yielded a bacterial strain, YZU1, with an impressive capacity to decolorize Reactive Black 5 (RB-5). *Bacillus* sp. YZU1 thrived on 100 mg/L of the dye, achieving 95% decolorization after 120 h. It was also able to tolerate up to 500 mg/L of RB-5. A Haldane model fitting yielded a maximum

degradation rate or q_{max} of 4.1549 h^{-1} at 283.6 mg/L of the dye [48]. In another study, *Alcaligenes faecalis* LJ-3 was able to completely degraded Acid Scarlet 3R concentration of 1000 mg/L within 16 h. The effect of the dye on dye degradation rate was modelled using the Michaelis-Menten model (Monod) giving a q_{max} of 115.90 h^{-1} and substrate concentration giving half q_{max} or K_s of 1193.23 mg/L [49].

Many studies only use either the Haldane or the Monod model for modelling. There are a few studies including this study that utilizes a comprehensive modelling approach to benefit the flexibility offered by other models. In one such study, Several inhibition kinetic models, including the Haldane, Monod, Luong, Aiba, Teissier-Edwards, Han-Levenspiel, and Yano models, were used to simulate the inhibitory effect of azo blue dye on its biodegradation by *Streptomyces* sp. DJP15. Only the Luong model did not adequately match the data, as shown by the results. The best model was Monod. The maximum specific degradation rate q_{max} was 0.431 h^{-1} and substrate concentration producing half maximal rate, or K_s value of 0.0001 (mg/L) [50]. In another study,

Crystal violet or gentian violet or basic violet 3 (BV) biodegradation by *Staphylococcus aureus* was modelled by a number of secondary models including Monod, Haldane, Teissier, Aiba, Yano and Koga, Hans-Levenspiel, Webb, and the Luong model. According to the result, Teissier was the most effective model. The results of these experiments suggest that BV is hazardous and reduces the pace of decolorization at greater dosages. The maximum BV specific biodegradation rate (q_{max}), half-saturation concentration (K_s), half inhibition concentration (K_i) were 0.145 h^{-1} , 0.408 mg/L and 73.205 mg/L, respectively [12]. The use of a comprehensive modelling approach can give better curve fitting results than a few popular models and should be the norm.

CONCLUSION

In conclusion, after conducting a comprehensive analysis that included various statistical metrics such as the corrected AICc (Akaike Information Criterion), bias factor (BF), adjusted coefficient of determination (R^2), and root-mean-square error (RMSE), it has been determined that the Monod model stands out as the most suitable model for describing the growth of *Acinetobacter baumannii* YNWH 226 during the degradation process of the Azo dye Congo red. This model's superiority was clearly evident through these statistical assessments. From the fitting exercise, we were able to extract valuable parameters for the Luong model, which was the best model based on statistical tests. These values provide a solid foundation for predicting the growth requirements of *Acinetobacter baumannii* YNWH 226 in the context of remediating Azo dye Congo red contamination in the environment. This knowledge will be instrumental in designing effective strategies for addressing environmental contamination and further advancing our understanding of microbial processes in environmental remediation.

REFERENCES

1. Yaseen DA, Scholz M. Textile dye wastewater characteristics and constituents of synthetic effluents: a critical review. Vol. 16, International Journal of Environmental Science and Technology. Springer Berlin Heidelberg; 2019. 1193–1226 p.
2. Saratale, G.D. et al. Dye wastewater treatment: A critical review on current treatment technologies. Environ Sci Pollut Res. 2009;2(16):103–18.
3. Azanaw A, Birlie B, Teshome B, Jemberie M. Textile effluent treatment methods and eco-friendly resolution of textile wastewater. Case Stud Chem Environ Eng. 2022;6(May):100230.

4. Mahar, R.B. et al. 2012. Textile dyeing industry an environmental hazard. *Nat Sci.* 2012;04(01):22–6.
5. Sreedharan V, Saha P, Rao KVB. Dye degradation potential of *Acinetobacter baumannii* strain VITVB against commercial azo dyes. *Bioremediation J.* 2021;25(4):347–68.
6. Gusmanizar N, Halmi MIE, Rusnam M, Rahman MFA, Shukor MS, Azmi NS, et al. Isolation and characterization of a molybdenum-reducing and azo-dye decolorizing *Serratia Marcescens* strain neni-1 from Indonesian soil. *J Urban Environ Eng.* 2016;10(1):113–23.
7. Sabo IA, Yahuza S, Shukor MY. Mathematical Modeling of the growth of *Acinetobacter baumannii* YNWH 226 on Azo dye Congo red. *J Environ Bioremediation Toxicol.* 2021;4(2):7–10.
8. Jung J, Park W. *Acinetobacter* species as model microorganisms in environmental microbiology: current state and perspectives. *Appl Microbiol Biotechnol.* 2015;99(6):2533–48.
9. Li R, Ning X an, Sun J, Wang Y, Liang J, Lin M, et al. Decolorization and biodegradation of the Congo red by *Acinetobacter baumannii* YNWH 226 and its polymer production's flocculation and dewatering potential. *Bioresour Technol.* 2015;194:233–9.
10. Ning XA, Yang C, Wang Y, Yang Z, Wang J, Li R. Decolorization and biodegradation of the azo dye Congo red by an isolated *Acinetobacter baumannii* YNWH 226. *Biotechnol Bioprocess Eng.* 2014;19(4):687–95.
11. Harumain ZAS, Mohamad MAN, Nordin NFH, Shukor MYA. Biodegradation of Petroleum Sludge by *Methylobacterium* sp. Strain ZASH. *Trop Life Sci Res.* 2023 Jul 21;34(2):197–222.
12. Manogaran M, Habib NMSA, Shukor MY, Yasid NA. Mathematical Modeling of Substrate Inhibition Kinetics of *Staphylococcus aureus* Growth on Basic Violet 3. *Bioremediation Sci Technol Res.* 2022 Dec 31;10(2):50–5.
13. Abubakar A, Gusmanizar N, Rusnam M, Syed MA, Shamaan NA, Shukor MY. Remodelling the Growth Inhibition Kinetics of *Pseudomonas* sp. Strain DrY Kertih on Acrylamide. *Bioremediation Sci Technol Res.* 2020 Dec 31;8(2):16–20.
14. Halmi MIE, Abdullah SRS, Johari WLW, Ali MSM, Shaharuddin NA, Khalid A, et al. Modelling the kinetics of hexavalent molybdenum (Mo6+) reduction by the *Serratia* sp. strain MIE2 in batch culture. *Rendiconti Lincei.* 2016 Dec 1;27(4):653–63.
15. Sabo IA, Yahuza S, Shukor MY. Molybdenum Blue Production from *Serratia* sp. strain DRY5: Secondary Modeling. *Bioremediation Sci Technol Res.* 2021 Dec 31;9(2):21–4.
16. Najim AA, Ismail ZZ, Hummadi KK. Biodegradation potential of sodium dodecyl sulphate (SDS) by mixed cells in domestic and non-domestic actual wastewaters: Experimental and kinetic studies. *Biochem Eng J.* 2022 Mar 1;180:108374.
17. Zhao H, Zhu J, Liu S, Zhou X. Kinetics study of nicosulfuron degradation by a *Pseudomonas nitroreducens* strain NSA02. *Biodegradation.* 2018;29(3):271–83.
18. Min J, Wang J, Chen W, Hu X. Biodegradation of 2-chloro-4-nitrophenol via a hydroxyquinol pathway by a Gram-negative bacterium, *Cupriavidus* sp. strain CNP-8. *AMB Express.* 2018 Mar 20;8(1):43.
19. Wen ZD, Gao DW, Wu WM. Biodegradation and kinetic analysis of phthalates by an *Arthrobacter* strain isolated from constructed wetland soil. *Appl Microbiol Biotechnol.* 2014;98(10):4683–90.
20. Basak SP, Sarkar P, Pal P. Isolation and characterization of phenol utilizing bacteria from industrial effluent-contaminated soil and kinetic evaluation of their biodegradation potential. *J Environ Sci Health - Part ToxicHazardous Subst Environ Eng.* 2014;49(1):67–77.
21. Rohatgi A. WebPlotDigitizer User Manual 4.3. [Http://rohatgi.info/WebPlotDigitizerapp](http://rohatgi.info/WebPlotDigitizerapp) Accessed June 2 2014. 2020;1–17.
22. Yahuza S, Dan-iyi BI, Sabo IA. Modelling the Growth of *Enterobacter* sp. on Polyethylene. *J Biochem Microbiol Biotechnol.* 2020;8(1):42–6.
23. Sabo IA, Yahuza S, Shukor MY. Molybdenum Blue Production from *Serratia* sp. strain DRY5: Secondary Modeling. *Bioremediation Sci Technol Res.* 2021;9(2):21–4.
24. Wayman M, Tseng MC. Inhibition-threshold substrate concentrations. *Biotechnol Bioeng.* 1976;18(3):383–7.
25. Akaike H. Making statistical thinking more productive. *Ann Inst Stat Math.* 2010;62(1):3–9.
26. Kass RE, Raftery AE. Bayes Factors. *J Am Stat Assoc.* 1995 Jun 1;90(430):773–95.
27. Burnham KP, Anderson DR. *Model Selection and Multimodel Inference: A Practical Information-Theoretic Approach.* Springer Science & Business Media; 2002. 528 p.
28. Ross T, McMeekin TA. Predictive microbiology. *Int J Food Microbiol.* 1994;23(3–4):241–64.
29. Zhou K, George SM, Métris A, Li PL, Baranyi J. Lag phase of *Salmonella enterica* under osmotic stress conditions. *Appl Environ Microbiol.* 2011;77(5):1758–62.
30. Zhao J, Gao J, Chen F, Ren F, Dai R, Liu Y, et al. Modeling and predicting the effect of temperature on the growth of *Proteus mirabilis* in chicken. *J Microbiol Methods.* 2014;99(1):38–43.
31. Velugoti PR, Bohra LK, Juneja VK, Huang L, Wesseling AL, Subbiah J, et al. Dynamic model for predicting growth of *Salmonella* spp. in ground sterile pork. *Food Microbiol.* 2011;28(4):796–803.
32. McElroy DM, Jaykus LA, Foegeding PM. Validation and analysis of modeled predictions of growth of *Bacillus cereus* spores in boiled rice. *J Food Prot.* 2000;63(2):268–72.
33. Kowalik J, Lobacz A, Tarczynska AS, Ziajka S. Graphical validation of growth models for *Listeria monocytogenes* in milk during storage. *Milchwissenschaft.* 2012;67(1):38–42.
34. Jung SH, Park SJ, Chun HH, Song KB. Effects of combined treatment of aqueous chlorine dioxide and fumaric acid on the microbial growth in fresh-cut paprika (*capsicum annum* L.). *J Appl Biol Chem.* 2014;57(1):83–7.
35. Huang L, Hwang CA, Phillips J. Evaluating the Effect of Temperature on Microbial Growth Rate-The Ratkowsky and a Bělehrádek-Type Models. *J Food Sci.* 2011;76(8):M547–57.
36. Monod J. The Growth of Bacterial Cultures. *Annu Rev Microbiol.* 1949;3(1):371–94.
37. Boon B, Laudelout H. Kinetics of nitrite oxidation by *Nitrobacter winogradskyi*. *Biochem J.* 1962;85:440–7.
38. Teissier G. Growth of bacterial populations and the available substrate concentration. *Rev Sci Instrum.* 1942;3208:209–14.
39. Aiba S, Shoda M, Nagatani M. Kinetics of product inhibition in alcohol fermentation. *Biotechnol Bioeng.* 1968 Nov 1;10(6):845–64.
40. Yano T, Koga S. Dynamic behavior of the chemostat subject to substrate inhibition. *Biotechnol Bioeng.* 1969 Mar 1;11(2):139–53.
41. Han K, Levenspiel O. Extended Monod kinetics for substrate, product, and cell inhibition. *Biotechnol Bioeng.* 1988;32(4):430–7.
42. Luong JHT. Generalization of monod kinetics for analysis of growth data with substrate inhibition. *Biotechnol Bioeng.* 1987;29(2):242–8.
43. Moser A. Kinetics of batch fermentations. In: Rehm HJ, Reed G, editors. *Biotechnology.* VCH Verlagsgesellschaft mbH, Weinheim; 1985. p. 243–83.
44. Webb J. *Enzyme and metabolic inhibitors* [Internet]. New York: Academic Press; 1963. 984 p. Available from: <https://www.biodiversitylibrary.org/bibliography/7320>
45. Hinshelwood CN. *The chemical kinetics of the bacterial cell.* Clarendon Press, Gloucestershire, UK; 1946.
46. Chen G, An X, Feng L, Xia X, Zhang Q. Genome and transcriptome analysis of a newly isolated azo dye degrading thermophilic strain *Anoxybacillus* sp. *Ecotoxicol Environ Saf.* 2020 Oct 15;203:111047.
47. Gopinath KP, Asan Meera Sahib H, Muthukumar K, Velan M. Improved biodegradation of Congored by using *Bacillus* sp. *Bioresour Technol.* 2009 Jan 1;100(2):670–5.
48. Wang ZW, Liang JS, Liang Y. Decolorization of Reactive Black 5 by a newly isolated bacterium *Bacillus* sp. YZU1. *Int Biodeterior Biodegrad.* 2013 Jan 1;76:41–8.
49. Song XY, Liu FJ, Zhou HB, Yang HL. Biodegradation of Acid Scarlet 3R by a New Salt-tolerant Strain *Alcaligenes faecalis* LJ-3: Character, Enzyme and Kinetics Analysis. *Chem Biochem Eng Q.* 2018 Oct 13;32(3):371–81.
50. Uba G, Abubakar A, Ibrahim S. Optimization of Process Conditions for Effective Degradation of Azo Blue Dye by *Streptomyces* sp. DJP15: A Secondary Modelling Approach. *Bull Environ Sci Sustain Manag.* 2021 Dec 31;5(2):28–32.